

This is the submitted version of the following article: Abu Yazid, N; Barrena. R. and Sánchez, A. *The immobilization of proteases produced by SSF onto functionalized magnetic nanoparticles: application in the hydrolysis of different protein sources* in Journal of molecular catalysis B: enzymatic (Ed. Elsevier), vol. 133, suppl. 1 (Nov. 2016), p. S230-S242, which has been published in final form at

DOI 10.1016/j.molcatb.2017.01.009

© 2016. This manuscript version is made available under the CC-BY-NC-ND 4.0 license <http://creativecommons.org/licenses/by-nc-nd/4.0/>

1 **The immobilisation of proteases produced by SSF onto functionalized magnetic**
2 **nanoparticles: Application in the hydrolysis of different protein sources**

3
4
5 Noraziah Abu Yazid, Raquel Barrena, and Antoni Sánchez*

6
7 Composting Research Group

8 Department of Chemical, Biological and Environmental Engineering

9 Escola d'Enginyeria

10 Universitat Autònoma de Barcelona

11 08193-Bellaterra (Barcelona, Spain)

12
13 *Corresponding author:

14 Tel.: +34 935811019

15 Fax: +34 935812013

16 Email address: antoni.sanchez@uab.cat

17

18

19

20

21

22

23

24

25

26

27

28 **ABSTRACT**

29 Alkaline proteases produced from protein-rich waste (hair waste and soya residues)
30 by solid state fermentation (SSF) were immobilised onto functionalized magnetic iron oxide
31 nanoparticles (MNPs) using glutaraldehyde as a crosslinking agent. The covalent binding
32 method had a better immobilisation yield compared to simple adsorption, retaining 93%-96%
33 (459±106 U/mg nanoparticles, 319±34 U/mg nanoparticles) of hair waste and soya residues
34 proteases, respectively after crosslinking with 5% glutaraldehyde for 6 h. However, the
35 adsorption immobilisation yield was 47%-54% after 8 h for both proteases. MNPs and
36 immobilised proteases were characterized using transmission electron microscopy (TEM),
37 scanning electron microscopy (SEM), Fourier transform infrared spectroscopy (FT-IR) and
38 electron diffraction. Our results indicated successful crosslinking between the proteases and
39 amino-functionalized MNPs. **The operational stability (pH and temperature) and storage**
40 **stability of free and immobilised enzyme were also analysed.** Despite the fact that the
41 optimum pH of free and immobilised proteases was identical in the alkaline region, the
42 immobilised proteases reached their optimum condition at higher temperatures (~~40°C–60°C~~
43 **40 °C – 60 °C**). After 2 months of storage at ~~4°C~~ **4 °C**, the immobilised proteases showed
44 good stability, retaining more than 85% of their initial activity. The high magnetic response
45 of MNPs render an ease of separation and reusability, which contributes to the residual
46 activity of both immobilised proteases on MNPs ~~remained retaining~~ more than 60% of their
47 initial values after seven hydrolytic cycles. These results ~~resulted showed~~ the enhancement of
48 the stability of the crosslinking interactions between the proteases and nanoparticles. The
49 immobilised proteases were capable of hydrolysing ~~select selected~~ proteins (casein, oat bran
50 protein isolate, and egg white albumin). However, differences in the degree of hydrolysis
51 were observed, depending on the combination of the protease and type of substrate used.

52 *Keywords:* protease; protein-rich waste; solid state fermentation; hydrolysis; immobilisation

53 **1. Introduction**

54 Because of the proteolytic nature of alkaline proteases, they have been commercially
55 utilised for industrial applications, explicitly in the food, pharmaceutical, textile, detergent,
56 and leather industries [1,2]. Their specific role in protein hydrolysis has drawn worldwide
57 attention regarding the versatility of these enzymes for biotechnological applications.
58 Currently, the general cost of protease production is very high, considering the cost of
59 substrates, commercial media and maintenance of cultures used for inoculation. For this
60 reason, the need to develop novel processes with higher yields is highly recommended from a
61 commercial point of view [3].

62 Different options have been considered to reduce the cost and increase the utilization of
63 proteases. One of the most promising alternatives is solid state fermentation (SSF), which
64 allows the procurement of value-added products using inexpensive waste as a solid substrate.
65 SSF has been successfully applied in the production of proteases using protein-rich waste
66 without the need to inoculate a specific microorganism [4,5]. In addition to recycling the
67 abundant solid waste produced by industries as cheap substrates, SSF avoids the hassle of
68 maintaining cultures since microorganism can develop mutations over time [6].
69 Economically, no additional cost is required, as there is no restricted sterilized environment
70 required to produce proteases through SSF since a specific microorganism for inoculation is
71 not involved.

72 Apart from that, soluble proteases are susceptible to autolysis, which leads to their rapid
73 inactivation. The instability and lack of flexibility, reusability and recovery make their use a
74 challenge for commercialization. Therefore, the use of immobilisation enzymes offers an
75 attractive method in which immobilised enzymes have enhanced stability that allows for their
76 recyclability and simple recovery without contamination of the final product [7]. There are

77 five basic enzyme immobilisation methods, including simple adsorption, covalent binding,
78 encapsulation, crosslinking, and entrapment [8].

79 ~~Of all the methods, covalent binding provides firm binding between the enzyme and~~
80 ~~carrier and avoids enzyme, as it can be regulated by using specific functional groups (-NH₂,~~
81 ~~SH) to bind with the proteins. Of all the methods, covalent binding provides firm binding~~
82 ~~between the enzyme and carrier, thus avoiding enzyme leakage as it can be regulated by~~
83 ~~using specific functional groups (-NH₂, -SH) [9]. This method of immobilisation provides an~~
84 ~~efficient way to increase the stability and flexibility of enzyme reusability and recovery [10].~~
85 Coupling agents, such as glutaraldehyde, maleic anhydride and genipin, have been widely
86 used as their functional groups can interact with the functional groups of modified carriers
87 and proteins [10,11]. Glutaraldehyde can be used either to alter enzymes after immobilisation
88 or to activate the support for enzyme immobilisation. In addition, the use of glutaraldehyde
89 can increase protein stability, thus avoiding protease autolysis [2,12].

90 In recent years, the immobilisation of enzymes onto nanomaterials, particularly iron oxide
91 magnetic nanoparticles (MNPs), to form nanobiocatalysts has attracted much attention in
92 some fields of research, including biolabeling, bioseparation, biosensors, biofuel cells, and
93 environmental analysis [9,13]. The use of MNPs has been particularly attractive for
94 immobilisation because of their special characteristics, such as their high surface area, simple
95 manipulation and separation by the application of an external magnetic field,
96 biocompatibility, biodegradability, and low toxicity [10,14]. ~~There are several studies~~
97 ~~reporting the application of purified protease immobilised on magnetic supports [15–18];~~
98 ~~however there are only a few studies that have exploited MNPs for crude protease~~
99 ~~immobilisation and further use in protein hydrolysis and synthesis [19].~~

100 In this work, the use of relatively inexpensive enzyme preparative for immobilisation
101 onto functionalized MNPs and crosslinking with glutaraldehyde was assessed. The goal was

102 to test the viability of using low-cost proteases derived from animal (hair waste) and
103 vegetable (soy fibre residues) protein-rich waste that were produced by SSF after being
104 immobilised onto functionalized MNPs in the hydrolysis of different type of proteins. The
105 relative differences in terms of stability and reusability between the free and immobilised
106 enzymes were significant, exhibiting the feasibility of the immobilised enzymes produced in
107 this work. Also, the magnetic properties of the support render a convenient separation
108 between the substrate and the enzymes within the catalytic system.

109

110 **2. Materials and Methods**

111 *2.1 Material and reagents*

112 Ferric chloride ($\text{FeCl}_3 \cdot 6\text{H}_2\text{O}$), ferrous sulphate ($\text{FeSO}_4 \cdot 7\text{H}_2\text{O}$), (3-aminopropyl)-
113 triethoxysilane (3-APTES, 97%), glutaraldehyde solution (50%), cetyl-trimethyl-ammonium
114 bromide (CTAB), trichloroacetic acid (TCA), Folin-Ciocalteu reagent, casein from bovine
115 milk, and egg white albumin were obtained from Sigma-Aldrich (Spain). Oat bran containing
116 17.6% protein was purchased from a supermarket (Mercadona, Spain). Hair waste with a
117 protein content of 75.6% was obtained from the local tanning industry located in Igualada,
118 Barcelona, and soya fibre residues with a protein content of 25.1% were received from
119 Natursoy, Spain. β -mercaptoethanol, tricine sample buffer, 10%-20% Mini-PROTEAN gels,
120 and Coomassie 250 stain were purchased from Bio-Rad (Spain). All other chemicals were
121 from commercial sources and were of analytical grade.

122 *2.2 Preparation of the protease enzyme concentrates from protein-rich waste using SSF*

123 Two different sources of alkaline proteases were produced from protein-rich waste, hair
124 waste and soya fibre residues using solid state fermentation (SSF) as described elsewhere
125 [4,5]. Briefly, hair waste and soya fibre residues were individually mixed with anaerobically

126 digested sludge at a weight ratio of 1:2, and then, the mixtures were added to a bulking agent
127 (wood chips) at a volumetric ratio of 1:1. SSF was undertaken in triplicate using 10 L air-
128 tight reactors for approximately 1 to 3 weeks. Later, the proteases, Phw from hair waste and
129 Psr from soya fibre residues, were extracted from the reactors using Tris-HCl buffer (50 mM,
130 pH 8.1). The times for extracting proteases for different substrates were specified for each
131 case based on the maximum activity of the protease produced during SSF. Phw at day 14th
132 yielded 787±124 U/g DW, and Psr at day 4th yielded 634±24 U/g DW. The extracts were
133 ultrafiltrated through Amicon Ultra-15 centrifugal filter devices (Millipore, Ireland) with a
134 10kDa molecular weight cut-off (MWCO) prior to lyophilisation. The initial activities after
135 lyophilisation for Phw and Psr were 466 U/ml and 330 U/ml, respectively.

136 *2.3 Preparation of oat bran protein isolate (OBPI)*

137 The preparation of oat bran protein isolate (OBPI) was performed as described elsewhere
138 [20] with slight modifications. Briefly, oat bran was added to 1.0 M NaCl at a ratio of 1:8
139 (w/v), and the pH was adjusted to 9.5 using 1.0 M NaOH. The mixture was agitated for 30
140 min at room temperature. Then, the supernatant was collected after centrifuged at 5,000 x g
141 for 25 min at ~~4°C~~ 4 °C. The pH was adjusted to 4 with 1.0 M HCl prior to centrifugation at
142 5,000 x g for 40 min at ~~4°C~~ 4 °C. The supernatant was then discarded, and the protein isolate
143 was dissolved in Milli-Q water and adjusted to pH 7 with 0.1 M NaOH. The protein isolate
144 was lyophilised and stored at ~~-20°C~~ -20 °C for future use.

145 *2.4 Synthesis of amino-functionalized Fe₃O₄ magnetic nanoparticles (MNPs)*

146 Magnetic nanoparticles (MNPs) were synthesised by co-precipitation in water phase
147 [21,22] with slight modifications. A mixture of 25 mM ferrous sulphate and 50 mM of ferric
148 chloride were dissolved in 100 ml of Milli-Q water with the addition of 0.1% of CTAB as a
149 stabiliser. The mixture was stirred at ~~40°C~~ 40 °C for 1 hour under ~~a-the~~ nitrogen atmosphere.

150 Then, 125 ml of deoxygenated NaOH (0.5 M) was added dropwise to the mixture, and the
151 mixture was left for 1 hour at ~~40°C~~ 40 °C to let the solution chemically precipitate. The
152 resultant MNPs were separated magnetically and washed five times with Milli-Q water. The
153 recovered MNPs were dried overnight at ~~60°C~~ 60 °C.

154 The surface of the MNPs was modified using a silanization reaction. Approximately 0.61
155 g of MNPs was dispersed in a solution containing 3.05 ml of APTES, 0.763 ml of Milli-Q
156 water, and 45.75 ml of methanol. The mixture was ultrasonically agitated for 30 min. Then,
157 10 ml of glycerol was added and heated at ~~90°C~~ 90 °C for 6 h, and the mixture was stirred
158 until separation. The surface-modified MNPs were recovered by applying a magnet, and they
159 were washed three times with Milli-Q water.

160 *2.5 Immobilisation of alkaline proteases (Phw, Psr)*

161 ~~For immobilisation of surface modified MNPs, 1 ml of alkaline protease from hair waste~~
162 ~~(Phw) with an initial activity 466 U/ml or alkaline protease from soya residue (Psr) with an~~
163 ~~initial activity 330 U/ml was dispersed in 9 ml of Tris HCl buffer (pH 8.1) and mixed with~~
164 ~~100 mg of amino functionalized MNPs. The activation of the NH₂ groups in the nanoparticles~~
165 ~~was carried out by adding glutaraldehyde as a crosslinking agent at various concentrations~~
166 ~~(1%, 2.5%, and 5% (v/v)). The mixture was gently agitated at 4°C 4 °C for 8 h. Subsequently,~~
167 ~~the immobilised proteases were separated by a magnetic field, washed five times with Tris~~
168 ~~buffer (50 mM, pH 8.1) to remove any unbound glutaraldehyde and finally resuspended in 1~~
169 ~~ml of Tris buffer (50 mM, pH 8.1). The immobilised proteases were stored at 4°C 4 °C for~~
170 ~~future use.~~

171 To begin with immobilisation of protease onto surface-modified MNPs, 1 ml of alkaline
172 protease from hair waste (Phw) with an initial activity 466 U/ml and alkaline protease from
173 soya residue (Psr) with an initial activity 330 U/ml, respectively, was dissolved in 9 ml of
174 Tris-HCl buffer (pH 8.1). Then, 100 mg of amino-functionalized MNPs was dispersed into

175 the mixture. Afterwards, the activation of the NH₂ groups in the nanoparticles was carried out
 176 by adding glutaraldehyde as a crosslinking agent at various concentrations (1%, 2.5%, and
 177 5% (v/v)) in the mixtures, followed by gentle agitation at 4 °C for 8 h. Subsequently, the
 178 MNPs with the immobilised proteases (MNPs-protease) were separated by a magnetic field
 179 and washed five times with Tris buffer (50 mM, pH 8.1) to remove any unbound
 180 glutaraldehyde and enzyme. Finally, the MNPs-protease were resuspended in 1 ml of Tris
 181 buffer (50 mM, pH 8.1) and stored at 4 °C for further application.

182 For immobilisation via adsorption, approximately 100 mg of naked MNPs were dispersed
 183 in 9 ml of the Tris buffer solution (50 mM, pH 8.1). Then, 1 ml of free alkaline protease from
 184 hair waste (466 U/ml) or soya residue (330 U/ml) was added. The mixture was gently
 185 agitated at 4°C 4 °C for 8 h. Later, the immobilised proteases were magnetically separated
 186 and treated as previously described.

187 The immobilisation yield (%) and the amount of immobilised protease (Phw_{im}, P_{sr}_{im})
 188 loading on MNPs (U/mg) were calculated using following equations (Eqs. 1, 2) [15,23]:

$$189 \text{ Enzyme loading (U/mg)} = (U_i - U_{sp})/W \quad (1)$$

$$190 \text{ Immobilisation yield (\%)} = (U_i - U_{sp})/U_i \times 100 \quad (2)$$

191 Where U_i is the initial enzyme activity (U), U_f is the enzyme activity in the supernatant after
 192 immobilisation (U), and W is the weight of MNPs used for immobilisation (mg).

193 Furthermore, the immobilisation efficiency (%) and activity recovery (%) were calculated as
 194 follows (Eqs. 3, 4) [23]:

$$195 \text{ Efficiency (\%)} = (U_e/U_{imm}) \times 100 \quad (3)$$

$$196 \text{ Activity recovery (\%)} = (U_e/U_i) \times 100 \quad (4)$$

197 Where U_e is the activity of bound enzyme that is measured in the immobilisate (U), U_{imm} is
198 the immobilised enzyme activity determined from subtracting the remaining enzyme activity
199 in the supernatant from the initial activity (U).

200 *2.6 Characterization of the immobilised enzymes*

201 Functionalized MNPs before and after immobilisation were characterized using high
202 resolution transmission electron microscopy (HRTEM, JEM-2011/JEOL) and scanning
203 electron microscopy (SEM, Zeiss Merlin). The samples were prepared by placing a drop of
204 the sonicated solutions on a copper grid, and then, the samples were allowed to dry. Samples
205 with the immobilised enzyme were stained with uranyl acetate (2%) prior to analysis.
206 Functionalized nanoparticle immobilisation was then confirmed using Fourier Transform
207 Infrared spectroscopy (FT-IR, Bruker Tenser 27) within a range of 500-4,000 cm^{-1} .

208 *2.7 Stability of immobilised protease*

209 The storage stability was determined by maintaining the immobilised enzymes via
210 crosslinking and simple adsorption at ~~4°C~~ 4 °C for 60 days. The activity of the enzymes was
211 measured at day 0th as the initial activity, while the activity for the 60th and 7th days were used
212 as the final activity of the immobilised enzymes and free enzymes, respectively.

213 To study the operational stability, both immobilised and free enzymes were incubated for
214 1 h at various pH and temperature values according to the response surface of the central
215 composite design (CCD) performed using the Design-Expert software (version 6.0.6). The
216 CCD consisted of 13 experimental points, including five replications at the central point and
217 four star points ($\alpha = 1$). The pH was adjusted using the following buffers: acetic acid-sodium
218 acetate 1 M (pH 5), Tris-HCl 1 M (pH 8), and Na_2HPO_4 -NaOH 0.05 M (pH 11). Analysis of
219 variance (ANOVA) was conducted to determine the significance of the main effects.

220 ~~The residual activity of each factor tested was calculated by that assuming the initial~~
221 ~~activity of the immobilised or free enzyme was 100%.~~ The residual activity of each factor
222 was calculated by assuming that the initial activity of the immobilised or free enzyme is
223 100%.

224 *2.8 Reusability of immobilised protease*

225 The reusability of immobilised proteases from hair waste (Phw) and soya fibre residue
226 (Psr) was tested on casein as a model protein. The initial activities of the immobilised
227 enzymes were measured and compared with seven consecutive repeated uses of immobilised
228 enzymes under the assay conditions. After each cycle, immobilised enzymes were
229 magnetically separated and washed with Tris-HCl buffer (50 mM, pH 8.1). Then, they were
230 resuspended in fresh medium and incubated at ~~50°C~~ 50 °C for 120 min. The activity of
231 immobilised enzymes from the first batch was considered to be 100%.

232 *2.9 Application of immobilised proteases in protein hydrolysis*

233 Prior to hydrolysis, 4% (w/v) suspension of selected proteins (casein from bovine milk,
234 egg white albumin, and OBPI) in Tris-HCl buffer (50 mM, pH 8.1) were incubated at ~~50°C~~
235 50 °C for 15 min. Then, the reaction was initiated by adding 1 ml of free enzymes (330-460
236 U/ml) or 1 ml immobilised enzymes suspension (319-459 U/mg NP) into 9 ml of substrate.
237 The mixture was incubated in a water bath at ~~50°C~~ 50 °C with mechanical agitation at 100
238 rpm. An aliquot of ~~six~~ 6 ml was withdrawn at 0.5, 2, 4, 6, and 24 h. The free enzyme activity
239 was deactivated by heating the samples in boiling water for 15 min. Then, the samples were
240 cooled by placing the samples in a cold water bath for 15 min. Afterwards, the samples were
241 centrifuged at 5,000 x g for 15 min to separate any impurities or enzyme from the
242 hydrolysate. The immobilised enzyme was separated from the hydrolysate by a magnetic
243 drive. The hydrolysate was kept frozen at ~~-80°C~~ -80 °C prior to lyophilisation.

244 2.10 Analytical methods

245 2.10.1 Protease assay

246 The proteolytic activity of the free and immobilised protease was determined using
247 casein as a substrate according to method described by Alef and Nannipieri [24] with slight
248 modifications. Briefly, 1 ml of the enzyme extract (free enzyme) or 0.1 g of immobilised
249 protease in 0.9 ml of Tris buffer (pH 8.1) was added to 5 ml of a 2% (w/v) casein solution
250 and incubated at ~~50°C~~ 50 °C and 100 rpm for 1 hour. The reaction was terminated by adding
251 5 ml of 15% (w/v) TCA. The samples were centrifuged at 10,000 rpm for 10 min at ~~4°C~~ 4 °C.
252 An aliquot of 0.5 ml of the supernatant was added to the alkaline reagent prior to the addition
253 of 0.5 ml of 25% (v/v) Folin-Ciocalteu phenol reagent. The resulting solution was incubated
254 at room temperature in the dark for 1 h. The absorbance was measured at 700 nm using a
255 tyrosine standard. One unit of alkaline protease activity was defined as the liberation of 1 µg
256 of tyrosine per minute under the assay conditions. All activity tests were performed in
257 triplicate.

258 2.10.2 Total protein content determination

259 The total protein content was determined by the Lowry method [25] using bovine serum
260 albumin (BSA) as a standard. The absorbance was analysed at 750 nm using an UV-visible
261 spectrophotometer (Varian Cary 50).

262 2.10.3 Degree of hydrolysis

263 The degree of hydrolysis was determined by quantifying the soluble protein content after
264 precipitation with TCA [19,26]. 1ml of protein hydrolysate was mixed with 1 ml of 10%
265 (w/v) TCA and incubated at ~~37°C~~ 37 °C for 30 min to allow for precipitation. This was
266 followed by centrifugation (10,000 x g, 10 min). Then, the soluble protein content in the

267 supernatant was determined by the Lowry method [25], and it was expressed in milligrams.

268 The degree of hydrolysis (DH) was determined using the following equation (Eq.1):

269

$$270 \quad \text{DH(\%)} = \frac{\text{soluble protein content in 10\% TCA}}{\text{total protein content}} \times 100 \quad (5)$$

271

272 *2.10.4 Electrophoresis*

273 Tricine-SDS PAGE was used to observe the pattern of smaller proteins generated after
274 the hydrolysis reaction. Electrophoresis was performed using 10-20% Mini-PROTEAN Tris-
275 Tricine gels under denaturing and reducing conditions. The reduction was achieved by
276 heating the sample at ~~90°C~~ 90 °C for 5 min in the presence of β-mercaptoethanol (2% v/v).
277 The gel was fixed with methanol (40% v/v) and acetic acid (10% v/v) and subsequently
278 stained with Coomassie Brilliant Blue R-250. Then, the gel was destained with a solution
279 containing methanol, acetic acid, and water (20: 4: 26 v/v).

280

281 **3. Results and discussion**

282 *3.1 Immobilisation of Phw and Psr onto magnetic nanoparticles*

283 The Phw and Psr enzymes from SSF were immobilised onto magnetic nanoparticles via
284 simple adsorption and crosslinking with glutaraldehyde (GA). Both methods were carried out
285 for 8 h with the aim of investigating the effect of time and crosslinker concentration on
286 immobilisation (Fig. 1). **The simple adsorption yielded a maximum activity recovery of 28%**
287 **with an activity loading of 87±22 U/mg NP for Phw and of 33% Psr (activity loading of**
288 **70±17 U/mg NP) after 8 h of immobilisation (Fig. 1a, 1c). The immobilisation efficiency for**
289 **both Phw and Psr in simple adsorption increased during 8 h with a maximum of 60-61%**
290 **efficiency yield, while the maximum immobilisation yield in simple adsorption for both Phw**

291 and Psr were 47% and 54%, respectively (Fig. 1b, 1d). The surfaces of naked MNPs likely
292 possess high reactivity, which makes them susceptible to degradation under particular
293 environmental conditions. This fact could involve weaker binding forces that contribute to
294 the poor stability of the protein attachment's to the surface [9,27].

295 Immobilisation via the crosslinker showed good results for both enzymes studied (Phw
296 and Psr). The immobilisation yield increased according to the increase in the GA
297 concentration from 1%-5% up to 6 h; then, it decreased abruptly for Phw (Fig. 1b). ~~Only~~
298 ~~when 1% GA with Psr was used did the immobilisation yield continue to increase (Fig. 1b).~~
299 Only when using Psr with 1% GA, the immobilisation yield continues increasing (Fig. 1d).
300 Maximum activity recovery and immobilisation yields were obtained after 6 h of crosslinking
301 time, 90% and 96% respectively, which is (equivalent to an activity load of 459 ± 106 U/mg
302 NP) for Phw with 5% GA (Fig 1a, 1b). Similarly in Psr with 5% GA the maximum activity
303 recovery and immobilisation yield were 92% and 93%, respectively (equivalent to activity
304 loading of 319 ± 34 U/mg NP) (Fig. 1c, 1d). In addition, the immobilisation via crosslinker
305 was superior to simple adsorption as both of the enzymes (Phw, Psr) showed good
306 immobilisation efficiency in the range of 45% to 98% during 6 h of immobilisation time (Fig
307 1b, 1d). This indicated that the crosslinking time and GA concentration play an important role
308 during the immobilisation of enzymes in this study. As GA plays a role as a spacer arm for
309 the carriers by providing aldehyde groups to couple to free amine groups from the enzymes,
310 forming imines, it can also act as a denaturing agent [12]. Additionally, some studies
311 obtained different crosslinking times (between 1 h to 4 h) and GA concentrations (from 1% to
312 6%), implying good biocompatibility for these specific enzymes [12,21,28,29].

313 3.2 Characterization of the functionalized nanoparticles used for immobilisation

314 Transmission electronic microscopy (TEM) images of MNPs before and after
315 modification with APTES and after the enzymes immobilisation onto the activated surface

316 were compared (Fig. 2). The average particle size of naked MNPs slightly increased from
317 10.2 nm (Fig. 2a) to 16.1 nm (Fig. 2b) after surface modification with APTES. This effect has
318 been observed previously in other studies [30,31]. After surface modification with APTES,
319 fewer nanoparticle aggregates formed. As suggested previously [10], surface modifications of
320 magnetic nanoparticles can improve their solubility and help avoid aggregation of particles.
321 In Fig. 2c and Fig. 2d, a layer covering surface of MNPs upon immobilisation of the
322 proteases (Phw and Psr) can be seen. The thickness of this layer covering the surface of
323 MNPs was estimated to be approximately 5.1 nm for Psr and 8.4 nm for Phw, indicating an
324 increase in the size of the particles.

325 Based on electron diffraction analysis (Fig. 3) of the TEM images, the crystalline
326 structure of the particles was not affected by surface modifications. Fig. 3a shows a clear
327 loop, confirming the crystalline structure of MNPs. After surface modification by APTES or
328 CTAB as a stabilizer, the crystalline structure was not modified; however, the size of some
329 nanoparticles was enlarged, as observed in Fig. 3b and Fig. 3c. Once protease immobilisation
330 was performed, the structure of the nanoparticles became an amorphous structure, confirming
331 that the enzyme covered the surface of the nanoparticles (Fig. 3d). **The surface of the naked**
332 **MNPs and functionalized MNPs can be observed in SEM images (Fig. 4a and Fig. 4b). The**
333 **small and spherical particles with well-defined edges are observed as in other studies [32]. In**
334 contrast, in Fig. 4c and Fig. 4d, the edge surface of nanoparticles is smooth because they are
335 covered by the enzymes, indicating that the immobilisation of proteases onto functionalized
336 MNPs was successful.

337 The surface modification and immobilisation of proteases (Phw and Psr) onto
338 nanoparticles was confirmed by a comparison of the FT-IR spectra of naked MNPs,
339 functionalized MNPs, and Phw and Psr immobilised onto functionalized MNPs. The FT-IR
340 spectrum in Fig. 5A shows a strong absorption peak at 584 cm^{-1} , which could corresponds to

341 Fe-O, as indicated in other studies [33,34]. It has been suggested that this strong peak could
342 be due to the stretching vibration mode associated with metal-oxygen absorption. In this
343 region, the stretching vibration peaks related to metal (ferrites in particular) in the octahedral
344 and tetrahedral sites of the oxide structure were found [31]. In Fig. 5A, the peaks at $1,662\text{ cm}^{-1}$
345 1 and $3,444\text{ cm}^{-1}$ were due to the bending and stretching vibration of -OH, respectively [35].
346 After grafting with APTES, the characteristic peak of the Fe-O bond shifted from 584 cm^{-1} to
347 638 cm^{-1} and 640 cm^{-1} because of the formation of the Fe-O-Si bond (Fig. 5B, 5C, 5D). The
348 shifting of the absorption peaks to high wavenumbers is due to the greater electronegativity
349 of -Si(O-) compared to H, which contributes to the bond forces for Fe-O bonds [36].
350 Additional strong peaks at $1,039\text{ cm}^{-1}$, $1,035\text{ cm}^{-1}$, and $1,034\text{ cm}^{-1}$ correspond to the Fe-O-Si
351 bending vibrations, indicating that alkyl silanes are successfully attached to functionalized
352 MNPs (Fig. 5B, 5C, 5D). Additionally, the presence of silane groups was observed at 995 cm^{-1}
353 1 , 893 cm^{-1} , and 896 cm^{-1} and were from the stretching vibrations of the Si-OH and Si-O-Si
354 groups from APTES [35,36]. Characteristic peaks of the immobilised enzymes attached via
355 the crosslinker (Fig. 5C, 5D) were observed at $1,536\text{ cm}^{-1}$, $1,544\text{ cm}^{-1}$ and $1,630\text{ cm}^{-1}$ because
356 of the C=N and C=O absorption from the glutaraldehyde and NH_2 from the enzyme [29].
357 Small shifts in intensity from $2,928\text{ cm}^{-1}$ (Fig. 5B) to $2,991\text{ cm}^{-1}$ (Fig. 5C) and $2,984\text{ cm}^{-1}$
358 (Fig. 5D) correspond to the C-H stretching vibration from the methyl group [37], which
359 illustrated the effect before and after the immobilisation of the enzymes. Additionally, in Fig.
360 5C and Fig. 5D, there were broad and strong peaks at $3,325\text{ cm}^{-1}$ and $3,344\text{ cm}^{-1}$, which
361 indicated the vibration modes of the O-H and -NH groups from enzymes that interact with
362 nanoparticles, which has been suggested previously [19].

363 *3.3 Operational stability of immobilised Phw and Psr*

364 The operational stability in terms of temperature and pH is an important criterion in the
365 application of immobilised enzymes [2,38]. To study this factor (Phw_im, Psr_im), various

366 pH values (5 – 11) and temperatures (30°C–70°C 30 °C – 70 °C) were tested, and the results
 367 were compared with those of free enzymes (Phw_free, Psr_free). The results were analysed
 368 using analysis of variance (ANOVA) to indicate the significant factor influencing the stability
 369 of both enzymes. The ANOVA results in Table 1 show that the regression coefficients had a
 370 high statistical significance ($p < 0.05$) and show the values obtained for the coefficient of
 371 determination for both Phw_im and Psr_im (R^2 0.9730 and R^2 0.9733) and Phw_free and
 372 Psr_free (R^2 0.9723 and R^2 0.9712, respectively). The values indicated that the model of the
 373 immobilised enzymes could not explain only 2.7% of the variables behaviour, while with the
 374 free enzymes the value was 2.8-2.9%. For immobilised enzymes, the calculated F-value
 375 ($\alpha = 0.05$, $DOF = 4,3$) was 9.12 for the regression. This value was higher than the tabulated F-
 376 values (1.65, 1.85), indicating that the treatment differences were highly significant.
 377 Similarly, in free enzymes, the obtained F-values (2.90, 3.94) were less than the critical F-
 378 value ($F_{0.05(4,5)} = 5.19$), reflecting the significance of the model. The following Equations (6 –
 379 9) represent the second order polynomial model of the residual activity for the experimental
 380 data:

$$381 \text{ Residual Phw_im(\%)} = -407.2 + 56.5\text{pH} + 10.1\text{T} - 2.6\text{pH}^2 - 0.1\text{T}^2 - 0.16\text{pHT} \quad (6)$$

$$382 \text{ Residual Psr_im(\%)} = -275.9 + 41.8\text{pH} + 6.3\text{T} - 1.8\text{pH}^2 - 0.05\text{T}^2 - 0.17\text{pHT} \quad (7)$$

$$383 \text{ Residual Phw_free(\%)} = 22.2 + 2.5\text{pH} + 1.5\text{T} - 0.026\text{T}^2 \quad (8)$$

$$384 \text{ Residual Psr_free(\%)} = 66.4 + 1.04\text{pH} + 0.54\text{T} - 0.021\text{T}^2 \quad (9)$$

385 For free enzymes, the models were reduced by removing the interaction between pH and
 386 temperature, as it was not significant to the stability of the free enzymes.

387 Contour plots of the second order polynomial model were generated as a function of the
 388 independent variables of pH and temperature for immobilised and free enzymes. The contour
 389 plots of free Phw and Psr exhibited their stability under mesophilic conditions (30°C 30 °C to
 390 40°C 40 °C). Free enzymes were stable over a broad range of pH values (Fig. 6b, 6d), with no

391 optimum condition obtained in the range tested (pH 5-11). However, both of the immobilised
392 enzymes had improved the stability by achieving their optimum condition in the alkaline
393 region (pH 8 to 11) with thermophilic temperature stability ranging from 40°C 40 °C to 60°C
394 60 °C for immobilised Phw (Fig. 6a) and 40°C 40 °C to 55°C 55 °C for immobilised Psr (Fig.
395 6c).

396 *3.4 Storage stability of immobilised Phw and Psr*

397 Storage stability plays a crucial role in the use immobilised proteases, as the shelf life
398 determines the viability of an immobilised enzyme over time [39]. The storage stabilities of
399 enzymes immobilised via a crosslinker (Phw_GA and Psr_GA) and adsorption (Phw_adsorp
400 and Psr_adsorp) were tested by dispersing the immobilised enzymes in Tris buffer and
401 maintaining them at 4°C 4 °C for 60 days. Free enzymes (Phw_free and Psr_free) were used
402 as controls to monitor the durability of enzyme activity. Phw_free and Psr_free were not
403 stable in solution, as their activity decreased over time. This fact could be related to the
404 behaviour of the proteases, as they tend to autolyse themselves by nucleophilic attack on the
405 intermediate in a presence of water [1,40]. After 7 days of storage at 4°C 4 °C, the residual
406 activity of Phw_free and Psr_free was less than 17% (Table 2). There was a significant
407 decrease in the activity of the immobilised enzyme via adsorption over 60 days of storage,
408 with a residual activity of less than 45%. The weak bonding between the enzyme and
409 nanoparticles could induce partial desorption during the period of storage. Generally,
410 immobilisation via adsorption involves relatively weak interactions, such as electrostatic
411 interactions, hydrogen bonds, van der Waals forces and hydrophobic interactions, which tend
412 to strip off enzymes from the carrier easily, thus leading to a loss of activity and
413 contamination of the reaction media [9]. However, the enzymes immobilised via crosslinking
414 (Phw_GA and Psr_GA) retained 91% and 86% of their residual activity, respectively, after

415 60 days of storage at 4°C (Table 2). These results show that enzymes immobilised created by
416 crosslinking provide a distinctive advantage in stability over immobilised enzymes created by
417 adsorption at a longer duration of storage.

418 *3.5 Reusability of immobilised Phw and Psr*

419 For the sake of the cost-effective use of enzymes, reusability is a critical factor to
420 consider [41]. The reusability of immobilised Phw and Psr created using crosslinking was
421 evaluated in a repeated batch process using fresh casein as a model protein in each batch
422 cycle (Fig. 7). Both immobilised Phw and Psr retained 66% and 64% of their activity,
423 respectively, after 7 cycles, indicating a significant enhancement of the stability of the
424 crosslinking interaction between the proteases and nanoparticles. In this work, testing the
425 reusability was feasible, as the immobilised enzymes were easily separated by a magnetic
426 force.

427 *3.6 Application of immobilised Phw and Psr in the hydrolysis of proteins*

428 Casein has been used as a model protein to evaluate the degree of hydrolysis (DH) of
429 immobilised enzymes created via crosslinking and free Phw or Psr. The results of the
430 hydrolysis are shown in Fig. 8a. The DH of immobilised Phw (24%) was higher than that of
431 free Phw (15%) during the first 30 min of reaction time (Fig. 8a). **The maximum DH was**
432 **achieved after 24 h and was 80% for immobilised Phw and 40% for free Phw. Besides, the**
433 **residual activity of both immobilised Phw and Psr were stable for 24 h whereas the residual**
434 **activity of free Phw and Psr had decreased pronouncedly after 24 h at 50 °C indicating an**
435 **improvement of process efficiency and thermal stability of the immobilised enzymes [19].**
436 **The higher stability may be possibly due to the multipoint covalent binding of protease to the**
437 **solid support that limit the flexibility and conformational mobility of the enzyme, hence**
438 **inhibits unfolding or denaturation of the enzyme [42]. Likewise, the DH of immobilised Psr**

439 (12%) showed the same rate as that of free Psr (13%) and continued to increase over time
440 with a similar profile, reaching the maximum DH 30% in free Psr and 50% in immobilised
441 Psr after 24 h of reaction time. Thus, the immobilised enzymes in the present study could
442 enhance the ability of free enzymes to hydrolyse protein, as shown by the model protein,
443 reflecting that the active enzymes were successfully immobilised.

444 The effect of both proteases (Phw and Psr) was also evaluated in hydrolysis of the protein
445 source from animals (egg white albumin) and vegetables (oat bran protein isolate). The
446 hydrolysis of oat bran protein isolate (OBPI) corroborated the efficiency of immobilised Phw
447 and Psr, as they had a higher DH compared to free Phw and Psr over a longer duration (Fig.
448 8b). These results agree with those obtained using functionalized magnetite nanoparticles to
449 hydrolyse soya protein isolates and whey protein isolates [29,43]. It seems that Psr exhibited
450 a higher DH than (free and immobilised) Phw when using a vegetable protein source. In the
451 hydrolysis of egg white albumin, immobilised Psr reached a maximum DH 60% after 24 h
452 and free Psr achieved maximum DH 45% after 6 h, while Phw reached a maximum DH of
453 70% and 51% for immobilised and free Phw, respectively (Fig. 8c). Hence, the different
454 source of the proteases seems to be a distinct behaviour that depends on the substrate source;
455 in fact, it could determine the choice of enzymes according to the application, as suggested
456 by others [2].

457 SDS-PAGE of the hydrolysates from selected proteins (casein, OBPI, egg white albumin)
458 is shown in Fig. 9. The presence of several smaller peptides with low molecular weights
459 support the idea that proteins were hydrolysed by immobilised protease derived from an
460 animal source (Phw) and vegetable source (Psr). Similar profiles were obtained for both
461 immobilised enzymes (Phw and Psr), showing their ability to perform the reaction after being
462 grafted on nanoparticle surfaces created by crosslinking with glutaraldehyde.

463

464 **4. Conclusion**

465 Low-cost proteases obtained through the SSF of protein-rich wastes (hair waste and soya
466 fibre residues) were successfully immobilised onto functionalized MNPs over a relatively
467 short time. The ease of the separation and reusability of these enzymes in comparison with
468 free enzymes could be considered an advantage of their use in industrial processes.
469 Additionally, stability was enhanced from mesophilic to thermophilic conditions under
470 alkaline conditions, preventing autolysis of the enzymes and maintaining their initial
471 activities for 2 months with only 9%-14% activity loss. Immobilised Phw and Psr were able
472 to hydrolyse some proteins derived from plant and animal sources with a high degree of
473 hydrolysis, indicating that they are promising for immobilised enzyme applications in a wide
474 range of industrial processes.

475

476 **Acknowledgements**

477 The authors thank the Spanish Ministerio de Economía y Competitividad (Project
478 CTM2015-69513-R) for their financial support. N.A. Yazid thanks the Government of
479 Malaysia and University Malaysia Pahang for their financial support. Raquel Barrena is
480 grateful to TECNIOspring fellowship programme (no. TECSPR15-1-0051) co-financed by
481 the European Union through the Marie Curie Actions and ACCIÓ (Generalitat de Catalunya).

482

483 **References**

- 484 [1] M.B. Rao, A.M. Tanksale, M.S. Ghatge, V. V. Deshpande, Molecular and
485 biotechnological aspects of microbial proteases., *Microbiol. Mol. Biol. Rev.* 62 (1998)
486 597–635.
- 487 [2] O.L. Tavano, Protein hydrolysis using proteases: An important tool for food
488 biotechnology, *J. Mol. Catal. B Enzym.* 90 (2013) 1–11.

- 489 [3] A.K. Mukherjee, H. Adhikari, S.K. Rai, Production of alkaline protease by a
490 thermophilic *Bacillus subtilis* under solid-state fermentation (SSF) condition using
491 Imperata cylindrica grass and potato peel as low-cost medium: Characterization and
492 application of enzyme in detergent formulation, *Biochem. Eng. J.* 39 (2008) 353–361.
- 493 [4] J. Abraham, T. Gea, A. Sánchez, Potential of the solid-state fermentation of soy fibre
494 residues by native microbial populations for bench-scale alkaline protease production,
495 *Biochem. Eng. J.* 74 (2013) 15–19.
- 496 [5] N.A. Yazid, R. Barrena, A. Sánchez, Assessment of protease activity in hydrolysed
497 extracts from SSF of hair waste by and indigenous consortium of microorganisms,
498 *Waste Manag.* 49 (2016) 420–426.
- 499 [6] S.S. Kim, H.S. Lee, Y.S. Cho, Y.S. Lee, C.S. Bhang, H.S. Chae, S.W. Han, I.S.
500 Chung, D.H. Park, The effect of the repeated subcultures of *Helicobacter pylori* on
501 adhesion, motility, cytotoxicity, and gastric inflammation., *J. Korean Med. Sci.* 17
502 (2002) 302–306.
- 503 [7] C. Mateo, J.M. Palomo, G. Fernandez-Lorente, J.M. Guisan, R. Fernandez-Lafuente,
504 Improvement of enzyme activity, stability and selectivity via immobilization
505 techniques, *Enzyme Microb. Technol.* 40 (2007) 1451–1463.
- 506 [8] M. Asgher, M. Shahid, S. Kamal, H.M.N. Iqbal, Recent trends and valorization of
507 immobilization strategies and ligninolytic enzymes by industrial biotechnology, *J.*
508 *Mol. Catal. B Enzym.* 101 (2014) 56–66.
- 509 [9] J. Xu, J. Sun, Y. Wang, J. Sheng, F. Wang, M. Sun, Application of iron magnetic
510 nanoparticles in protein immobilization, *Molecules.* 19 (2014) 11465–11486.
- 511 [10] X. Jin, J.F. Li, P.Y. Huang, X.Y. Dong, L.L. Guo, L. Yang, Y.C. Cao, F. Wei, Y. Di
512 Zhao, H. Chen, Immobilized protease on the magnetic nanoparticles used for the
513 hydrolysis of rapeseed meals, *J. Magn. Magn. Mater.* 322 (2010) 2031–2037.
- 514 [11] I.A. Cavello, J.C. Contreras-Esquivel, S.F. Cavalitto, Immobilization of a keratinolytic
515 protease from *Purpureocillium lilacinum* on genipin activated-chitosan beads, *Process*
516 *Biochem.* 49 (2014) 1332–1336.
- 517 [12] H.J. Chae, M.J. In, E.Y. Kim, Optimization of protease immobilization by covalent
518 binding using glutaraldehyde., *Appl. Biochem. Biotechnol.* 73 (1998) 195–204.
- 519 [13] S.A. Ansari, Q. Husain, Potential applications of enzymes immobilized on/in nano
520 materials: A review, *Biotechnol. Adv.* 30 (2012) 512–523.
- 521 [14] P. Xu, G.M. Zeng, D.L. Huang, C.L. Feng, S. Hu, M.H. Zhao, C. Lai, Z. Wei, C.
522 Huang, G.X. Xie, Z.F. Liu, Use of iron oxide nanomaterials in wastewater treatment:
523 A review, *Sci. Total Environ.* 424 (2012) 1–10.
- 524 [15] A. Sahu, P.S. Badhe, R. Adivarekar, M.R. Ladole, A.B. Pandit, Synthesis of
525 glycinamides using protease immobilized magnetic nanoparticles, *Biotechnol. Reports.*
526 12 (2016) 13–25.

- 527 [16] S.-L. Cao, X.-H. Li, W.-Y. Lou, M.-H. Zong, Preparation of a novel magnetic
528 cellulose nanocrystal and its efficient use for enzyme immobilization, *J. Mater. Chem.*
529 *B.* 2 (2014) 5522–5530.
- 530 [17] S. Cao, H. Xu, X. Li, W. Lou, M. Zong, Papain@magnetic nanocrystalline cellulose
531 nanobiocatalyst: a highly efficient biocatalyst for dipeptide biosynthesis in deep
532 eutectic solvents, *ACS Sustain. Chem. Eng.* 3 (2015) 1589–1599.
- 533 [18] S. Cao, Y. Huang, X. Li, P. Xu, H. Wu, N. Li, W. Lou, Preparation and
534 Characterization of Immobilized Lipase from *Pseudomonas Cepacia* onto Magnetic
535 Cellulose Nanocrystals, *Sci. Rep.* 6 (2016) 1–12.
- 536 [19] R. Sinha, S.K. Khare, Immobilization of halophilic *Bacillus* sp. EMB9 protease on
537 functionalized silica nanoparticles and application in whey protein hydrolysis,
538 *Bioprocess Biosyst. Eng.* 38 (2015) 739–748.
- 539 [20] S. Jodayree, Antioxidant activity of oat bran hydrolyzed proteins in vitro and in vivo,
540 Doctoral Thesis, Ottawa, Ontario, 2014.
- 541 [21] T.G. Hu, J.H. Cheng, B.B. Zhang, W.Y. Lou, M.H. Zong, Immobilization of alkaline
542 protease on amino-functionalized magnetic nanoparticles and its efficient use for
543 preparation of oat polypeptides, *Ind. Eng. Chem. Res.* 54 (2015) 4689–4698.
- 544 [22] A. Abo Markeb, A. Alonso, A.D.A.D. Dorado, A. Sánchez, X. Font, Phosphate
545 removal and recovery from water using nanocomposite of immobilized magnetite
546 nanoparticles on cationic polymer, *Environ. Technol.* 3330 (2016) 1–14.
- 547 [23] R.A. Sheldon, S. Van Pelt, Enzyme immobilisation in biocatalysis: why, what and
548 how, *Chem. Soc. Rev.* 42 (2013) 6223–6235.
- 549 [24] K. Alef, P. Nannipieri, Methods in applied soil microbiology and biochemistry -
550 Enzyme activities, Academic Press, San Diego, 1995.
- 551 [25] O.H. Lowry, N.J. Rosebrough, A.L. Farr, R.J. Randall, Protein measurement with the
552 Folin phenol reagent., *J. Biol. Chem.* 193 (1951) 265–275.
- 553 [26] M.P.C. Silvestre, H.A. Morais, V.D.M. Silva, M.R. Silva, Degree of hydrolysis and
554 peptide profile of whey proteins using pancreatin, *Brazilian Soc. Food Nutr.* 38 (2013)
555 278–290.
- 556 [27] D.A. Cowan, R. Fernandez-Lafuente, Enhancing the functional properties of
557 thermophilic enzymes by chemical modification and immobilization, *Enzyme Microb.*
558 *Technol.* 49 (2011) 326–346.
- 559 [28] S. Prasertkittikul, Y. Chisti, N. Hansupalak, Deproteinization of natural rubber using
560 protease immobilized on epichlorohydrin cross-linked chitosan beads, *Ind. Eng. Chem.*
561 *Res.* 52 (2013) 11723–11731.
- 562 [29] S.N. Wang, C.R. Zhang, B.K. Qi, X.N. Sui, L.Z. Jiang, Y. Li, Z.J. Wang, H.X. Feng,
563 R. Wang, Q.Z. Zhang, Immobilized alcalase alkaline protease on the magnetic chitosan

- 564 nanoparticles used for soy protein isolate hydrolysis, *Eur. Food Res. Technol.* 239
565 (2014) 1051–1059.
- 566 [30] H. Quanguo, Z. Lei, W. Wei, H. Rong, H. Jingke, Preparation and Magnetic
567 Comparison of Silane-Functionalized Magnetite Nanoparticles, 22 (2010) 285–295.
- 568 [31] J.A. Lopez, F. González, F.A. Bonilla, G. Zambrano, M.E. Gómez, Synthesis and
569 characterization of Fe₃O₄ magnetic nanofluid, *Rev. Latinoam. Metal. Y Mater.* 30
570 (2010) 60–66.
- 571 [32] M.R. Ladole, A.B. Muley, I.D. Patil, M.I. Talib, R. Parate, Immobilization of
572 tropizyme-P on amino-functionalized magnetic nanoparticles for fruit juice
573 clarification, *J. Biochem. Tech.* 5 (2014) 838–845.
- 574 [33] I.J. Bruce, T. Sen, Surface modification of magnetic nanoparticles with alkoxy silanes
575 and their application in magnetic bioseparations, *Langmuir.* 21 (2005) 7029–7035.
- 576 [34] M. Yamaura, R.L. Camilo, L.C. Sampaio, M.A. Macedo, M. Nakamura, H.E. Toma,
577 Preparation and characterization of (3-aminopropyl)triethoxysilane-coated magnetite
578 nanoparticles, *J. Magn. Magn. Mater.* 279 (2004) 210–217.
- 579 [35] D.L. Pavia, G.M. Lampman, G.S. Kriz, J.A. Vyvyan, eds., Introduction to
580 spectroscopy, 5th ed., Cengage Learning, United State of America, 2015.
- 581 [36] R.A. Bini, R.F.C. Marques, F.J. Santos, J.A. Chaker, M. Jafelicci, Synthesis and
582 functionalization of magnetite nanoparticles with different amino-functional
583 alkoxy silanes, *J. Magn. Magn. Mater.* 324 (2012) 534–539.
- 584 [37] P.E.G. Casillas, C.A.R. Gonzalez, C.A.M. Pérez, Infrared Spectroscopy of
585 Functionalized Magnetic Nanoparticles, in: T. Theophile (Ed.), *Infrared Spectrosc. -*
586 *Mater. Sci. Eng. Technol.*, InTech, 2012: pp. 405–420.
- 587 [38] R.J.S. De Castro, H.H. Sato, Production and biochemical characterization of protease
588 from *Aspergillus oryzae*: An evaluation of the physical-chemical parameters using
589 agroindustrial wastes as supports, *Biocatal. Agric. Biotechnol.* 3 (2014) 20–25.
- 590 [39] A.G. Kumar, S. Swarnalatha, P. Kamatchi, G. Sekaran, Immobilization of high
591 catalytic acid protease on functionalized mesoporous activated carbon particles,
592 *Biochem. Eng. J.* 43 (2009) 185–190.
- 593 [40] R. Beynon, J.S. Bond, eds., *Proteolytic enzymes: a practical approach*, 3rd ed., Oxford
594 University Press, 2001.
- 595 [41] T. Chen, W. Yang, Y. Guo, R. Yuan, L. Xu, Y. Yan, Enhancing catalytic performance
596 of β -glucosidase via immobilization on metal ions chelated magnetic nanoparticles,
597 *Enzyme Microb. Technol.* 63 (2014) 50–57.
- 598 [42] R.K. Singh, Y.W. Zhang, N.P.T. Nguyen, M. Jeya, J.K. Lee, Covalent immobilization
599 of beta-1,4-glucosidase from *Agaricus arvensis* onto functionalized silicon oxide
600 nanoparticles, *Appl. Microbiol. Biotechnol.* 89 (2011) 337–344.

601 [43] E.M. Lamas, R.M. Barros, V.M. Balcao, F.X. Malcata, Hydrolysis of whey proteins by
602 proteases extracted from *Cynara cardunculus* and immobilized onto highly activated
603 supports, *Enzyme Microb. Technol.* 28 (2001) 642–652.

604

605

606

607

608

609

610

611

612

613

614

615

616

617

618

619

620

621 **Tables**

622 **Table 1** Analysis of variance (ANOVA) for the response surface quadratic model for
 623 immobilised (Phw_im and Psr_im) and free (Phw_free and Psr_free) enzymes.

Protease	Source of variation	Sums of square	Degree of freedom	Mean square	F-value	Prob>F
Phw_im	Regression	12107.4	5	2421.5	50.47	<0.0001
	Residual	335.9	7	47.98		
	Pure error	150	4	37.5		
	Lack of fit	185.9	3	61.95	1.65	
	Total	12443.2	12			
Psr_im	Regression	5108.7	5	1021.7	50.99	<0.0001
	Residual	140.3	7	20		
	Pure error	58.8	4	14.7		
	Lack of fit	81.5	3	27.2	1.85	
	Total	5248.9	12			
Phw_free	Regression	3382.4	3	1127.5	105.4	<0.0001
	Residual	96.3	9	10.7		
	Pure error	20.8	4	5.2		
	Lack of fit	75.5	5	15.1	2.9	
	Total	3478.7	12			
Psr_free	Regression	6452.3	3	2150.8	101.1	<0.0001
	Residual	191.5	9	21.3		
	Pure error	32.3	4	8.1		
	Lack of fit	159.2	5	31.8	3.94	
	Total	6643.8	12			

624 Phw_im: R² 0.9730, adj R² 0.9537, pred R² 0.8519

625 Psr_im: R² 0.9733, adj R² 0.9542, pred R² 0.8260

626 Phw_free: R² 0.9723, adj R² 0.9631, pred R² 0.9315

627 Psr_free: R² 0.9712, adj R² 0.9616, pred R² 0.9224

628
 629
 630
 631
 632
 633
 634
 635
 636
 637
 638
 639
 640
 641
 642
 643
 644

645 **Table 2** The storage stability of free and immobilised enzymes created via crosslinking with
 646 glutaraldehyde (GA) and via adsorption (adsorp) during 60 days of storage.
 647

Enzymes	Initial activity (U/ml)	Final activity (U/ml)	Residual activity (%)
Phw_GA	501±72	458±51	91
Psr_GA	346±69	297±84	86
Phw_adsorp	190±15	77±9	41
Psr_adsorp	152±9	46±5	30
Phw_free	537±26	91±21 ^a	17
Psr_free	358±29	42±3 ^a	12

648 ^a The final activity was determined after 7 days of storage.
 649 The standard deviation was calculated from 3 replicates.

650
 651
 652
 653

654

655

656

657

658

659

660

661

662

663

664

665

666

667

668

669 **Figure captions**

670 **Fig. 1** The effect of the glutaraldehyde (GA) concentration and crosslinking time on the
 671 activity recovery of (a) Phw and (c) Psr with 0% GA (simple adsorption) (■), 1% GA (▨),
 672 2.5% GA (▩), and 5% GA (▧); enzyme loading per carrier of (a) Phw and (c) Psr with 0%
 673 GA (simple adsorption) (—●—), 1% GA (—○—), 2.5% GA (—▼—), and 5% GA (—△—);
 674 immobilisation yield of (b) Phw and (d) Psr with 0% GA (simple adsorption) (■), 1% GA (▨),
 675 2.5% GA (▩), and 5% GA (▧); immobilisation efficiency of (b) Phw and (d) Psr
 676 with 0% GA (simple adsorption) (—●—), 1% GA (—○—), 2.5% GA (—▼—), and 5% GA (—△—)
 677 —△—) onto amino-functionalized MNPs.

678 **Fig. 2** TEM images at a magnification of 30,000x of (a) naked MNPs, (b) amino-
 679 functionalized MNPs, (c) amino-functionalized MNPs after being immobilised with Phw, and
 680 (d) amino-functionalized MNPs after being immobilised with Psr.

681 **Fig. 3** The electron diffraction images of (a) naked MNPs, (b) MNPs after the addition of
 682 CTAB, (c) MNPs after surface modification with APTES, and (d) MNPs after the
 683 immobilisation of the enzymes Phw and Psr.

684 **Fig. 4** The SEM images at 50.00 KX magnification of (a) naked MNPs, (b) amino-
 685 functionalized MNPs, (c) amino-functionalized MNPs after being immobilised with Phw, and
 686 (d) amino-functionalized MNPs after being immobilised with Psr.

687 **Fig. 5** The FT-IR spectra of (A) naked MNPs, (B) amino-functionalized MNPs, (C) amino-
 688 functionalized MNPs after immobilisation of Phw, and (D) amino-functionalized MNPs after
 689 immobilisation of Psr.

690 **Fig. 6** Contour plots of the residual activity (%) of the enzymes in terms of their operation
 691 stability as a function of pH and temperature of (a) immobilised Phw, (b) free Phw, (c)
 692 immobilised Psr, and (d) free Psr

693 **Fig. 7** The reusability of immobilised Phw (■) and immobilised Psr (□) onto amino-
694 functionalized MNPs using casein as a model substrate for the hydrolysis reaction

695 **Fig. 8** The degree of hydrolysis of the selected protein hydrolysates obtained from the
696 hydrolysis of immobilised Phw (—○—), free Phw (—●—), immobilised Psr (—△—), and free Psr
697 (—▽—) with (a) casein; (b) oat bran protein isolate (OBPI); and (c) egg white albumin. The
698 residual activity of immobilised Phw (—□—), free Phw (—■—), immobilised Psr (—◇—) and
699 free Psr (—◆—) in 50 °C during 24h.

700 **Fig. 9** SDS-PAGE of the hydrolysates after reduction using 2-mercaptoethanol for selected
701 proteins before and after treatment with the immobilised proteases; (1) Molecular mass
702 marker; (2) casein; (3) egg white albumin; (4) hydrolysate from casein after treated with
703 immobilised Phw; (5) hydrolysate from egg white albumin after treatment with immobilised
704 Phw; (6) hydrolysate from OBPI after treatment with immobilised Phw; (7) hydrolysate from
705 casein after treatment with immobilised Psr; (8) hydrolysate from egg white albumin after
706 treatment with immobilised Psr; (9) hydrolysate from OBPI after treatment with Psr.

707

708

709

710

711

712

713

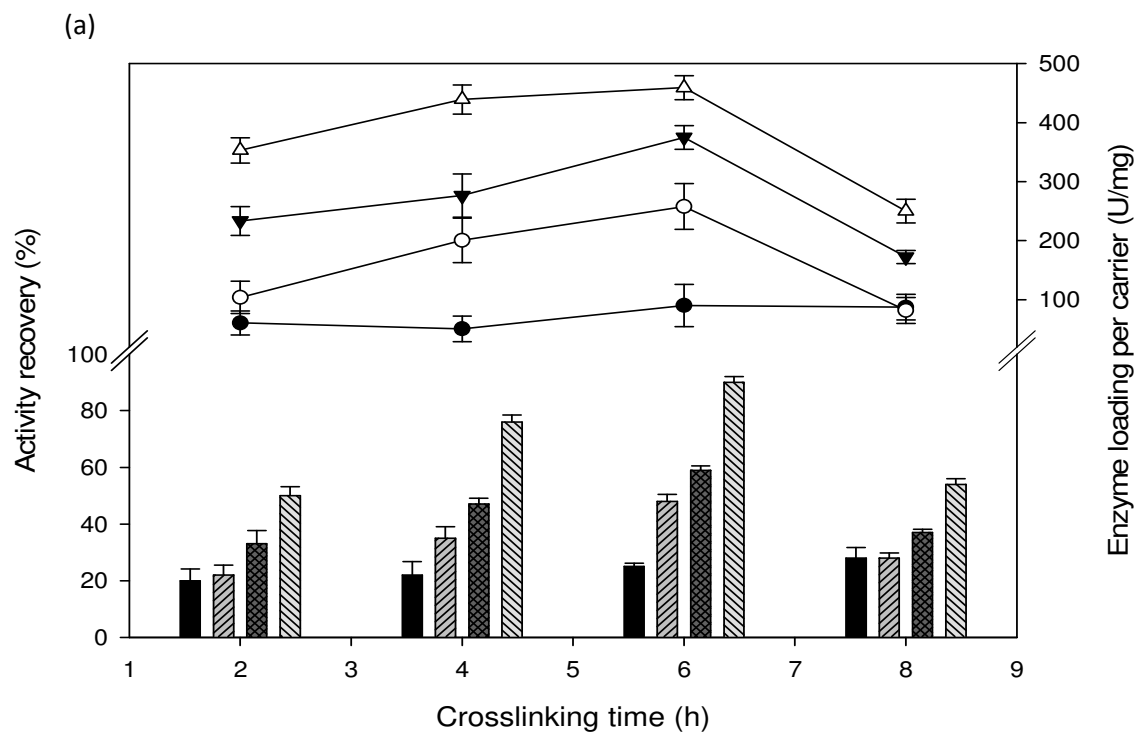
714

715

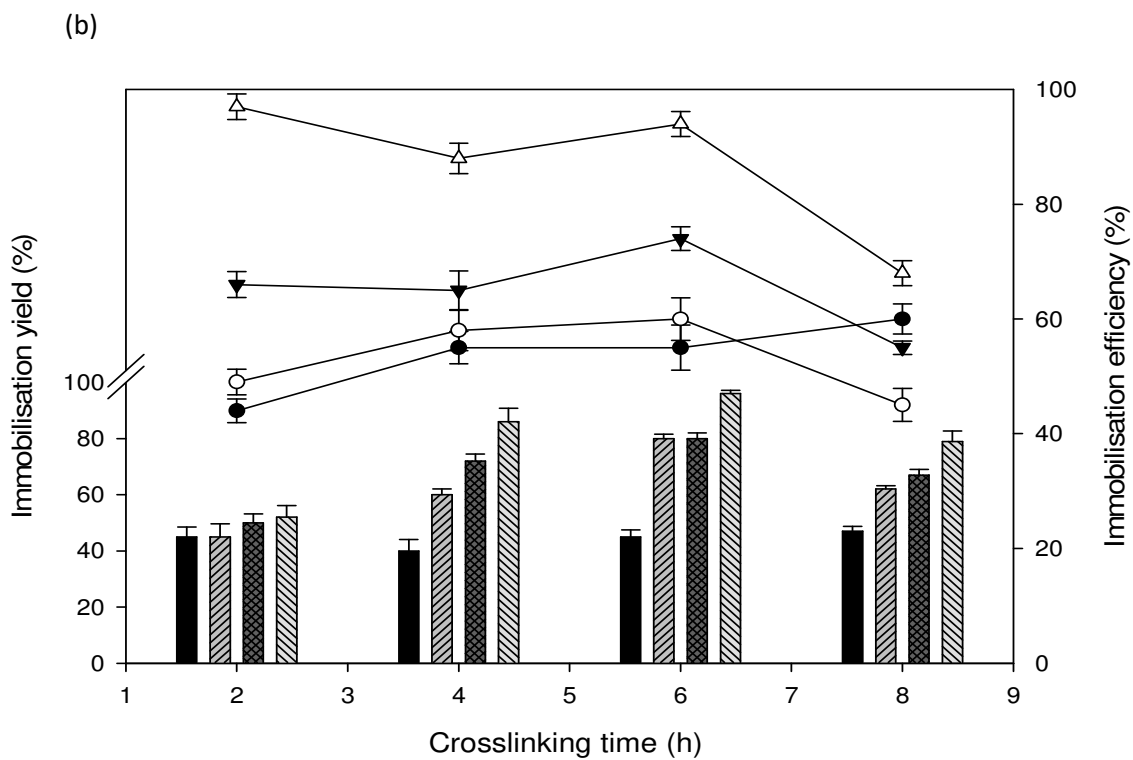
716

717

718 **Fig. 1**

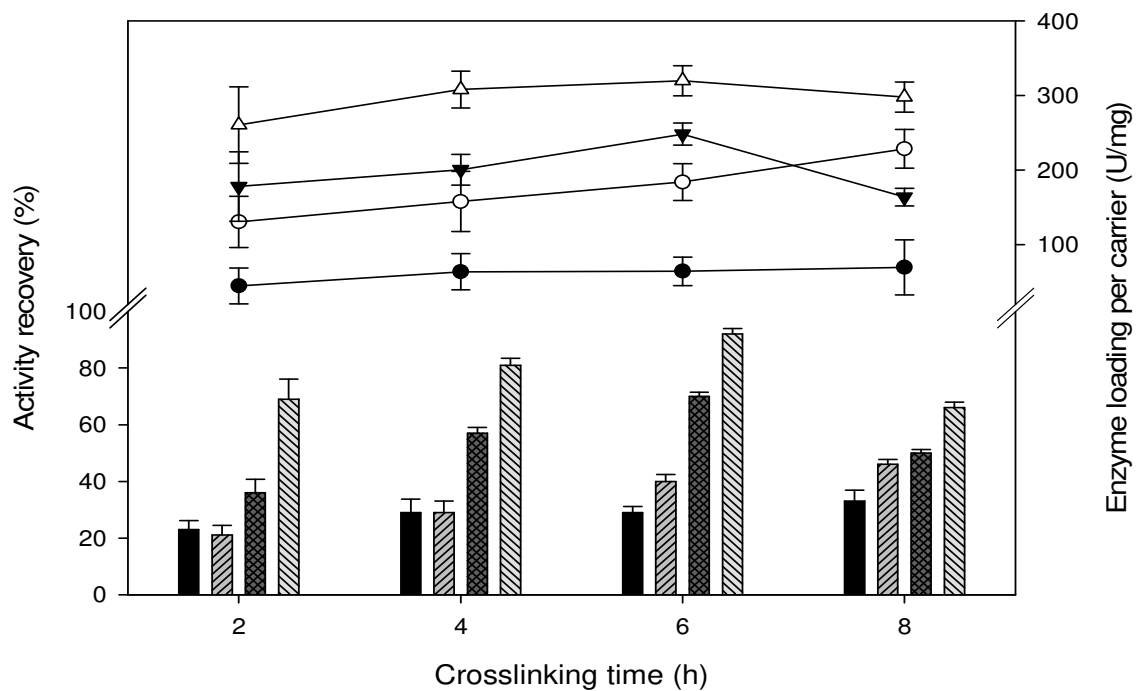


719



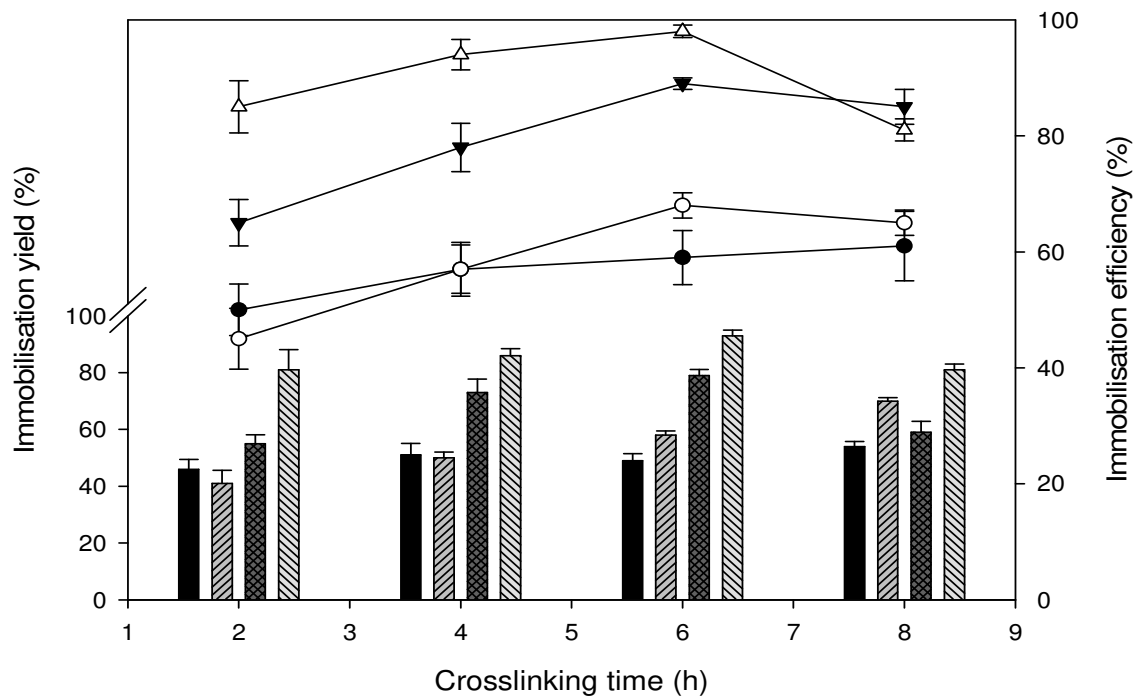
720

(c)



721

(d)



722

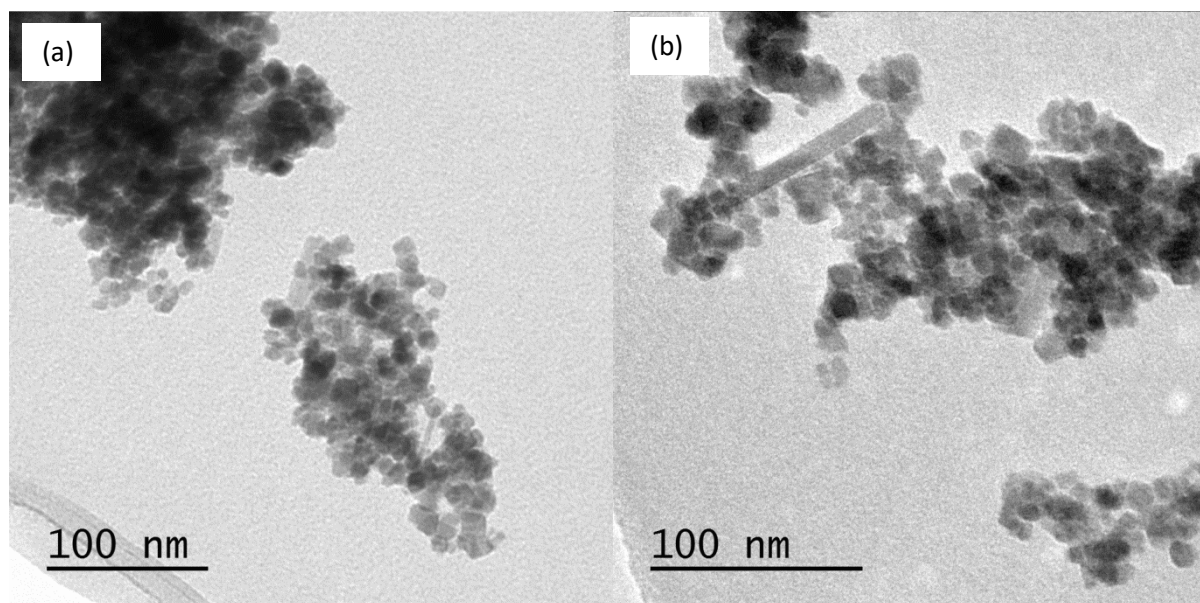
723

724

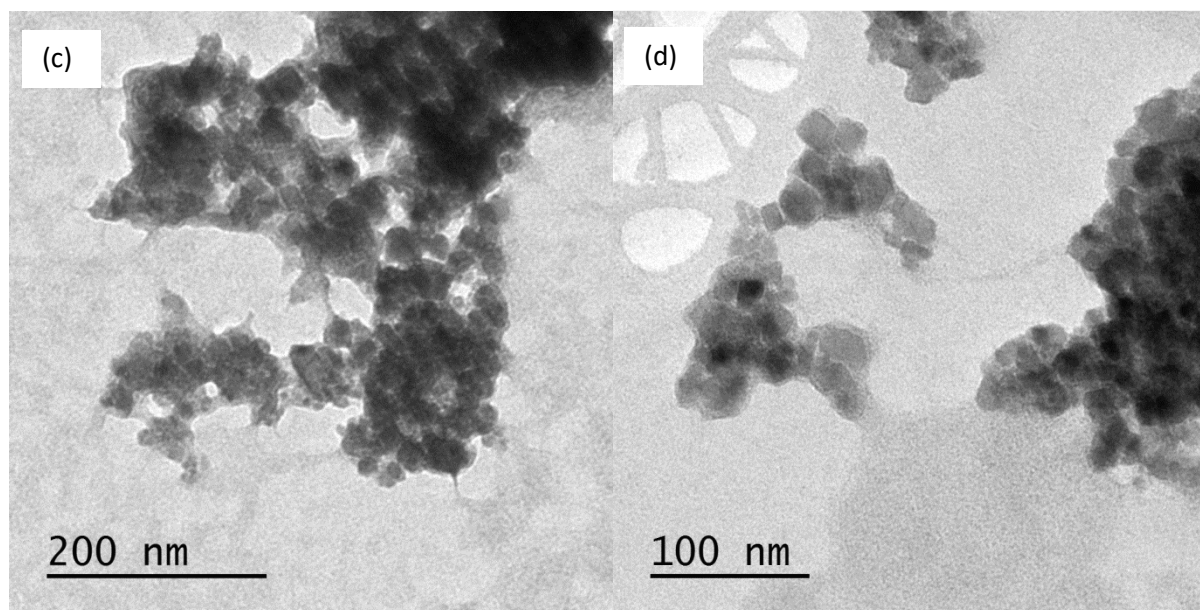
725

726

727 **Fig. 2**



728



729

730

731

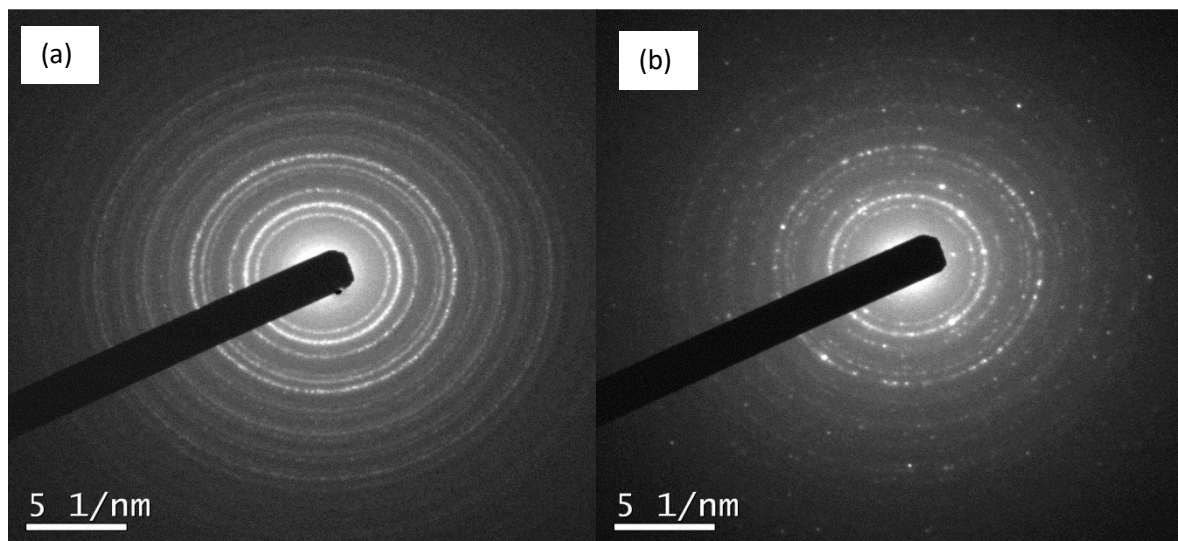
732

733

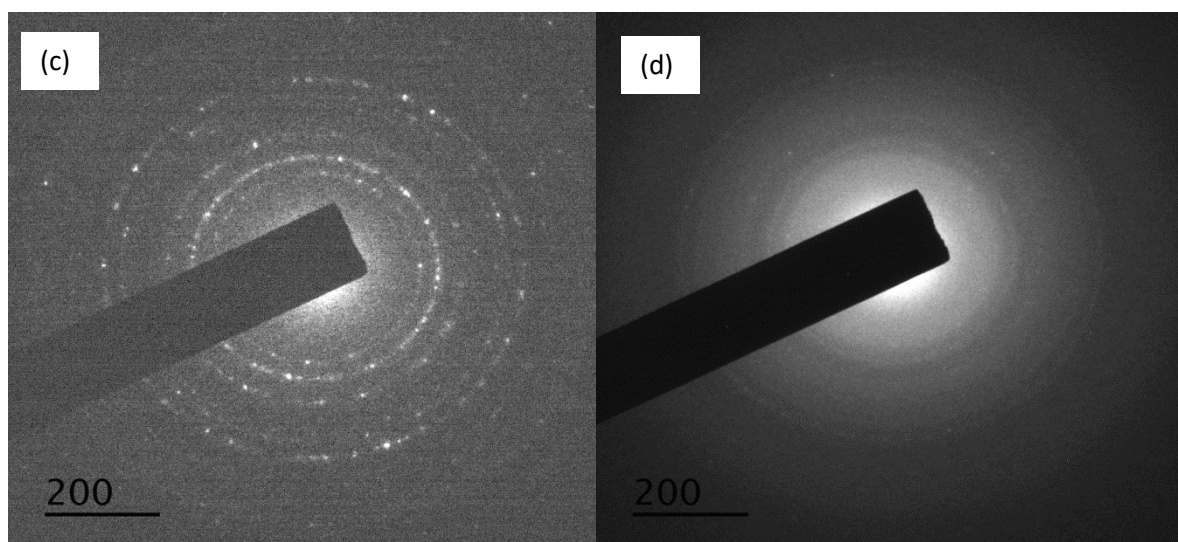
734

735

736

737 **Fig. 3**

738



739

740

741

742

743

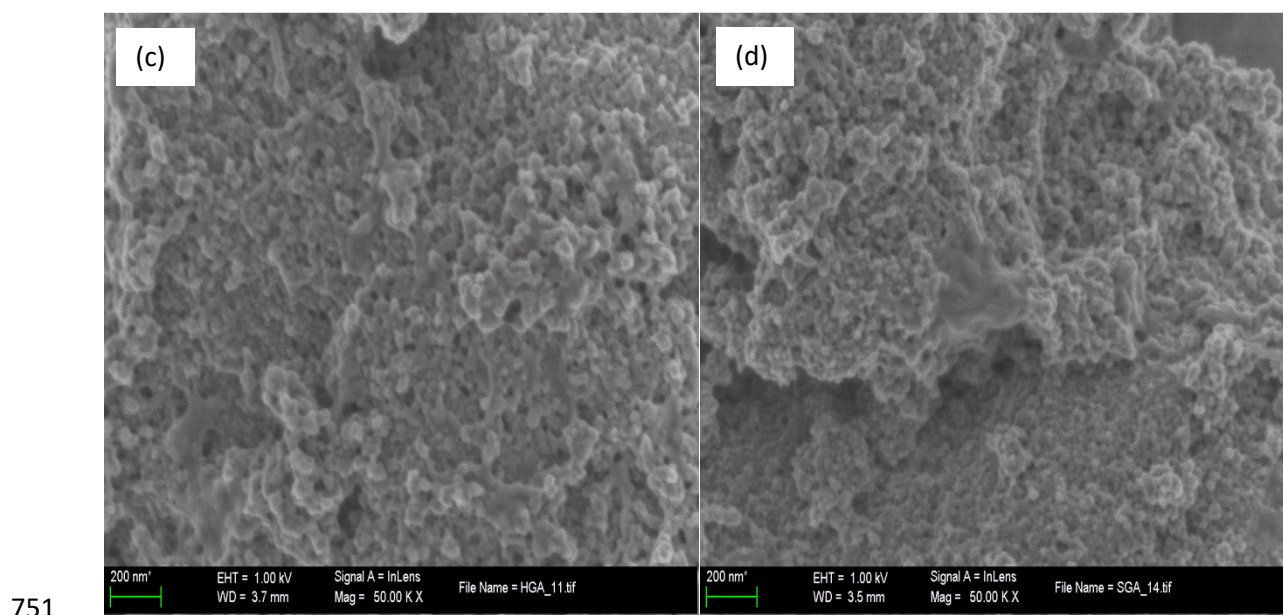
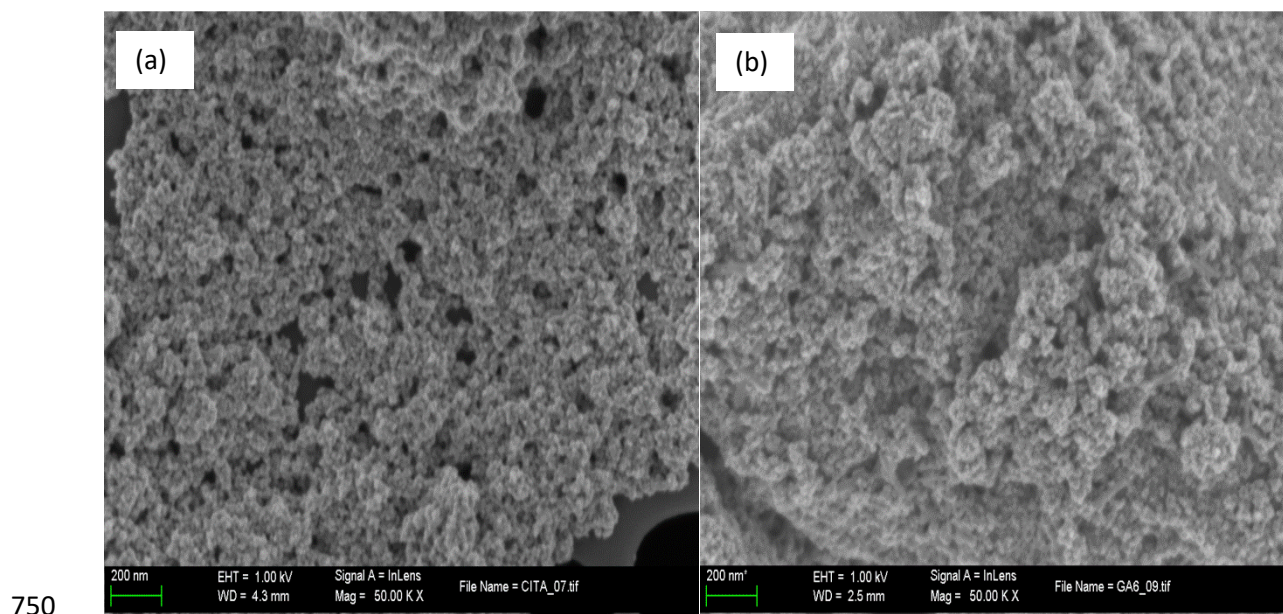
744

745

746

747

748

749 **Fig. 4**

752

753

754

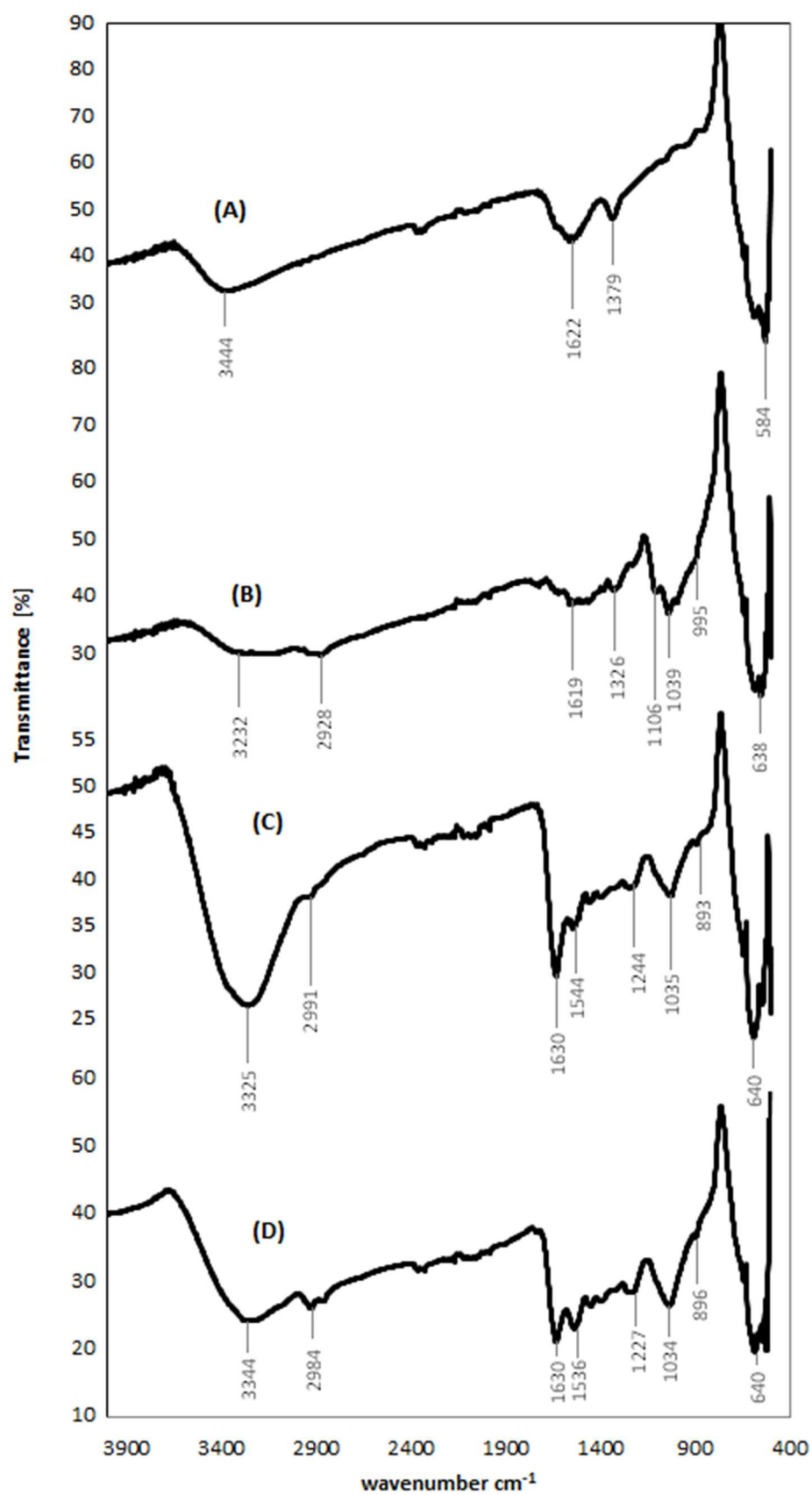
755

756

757

758

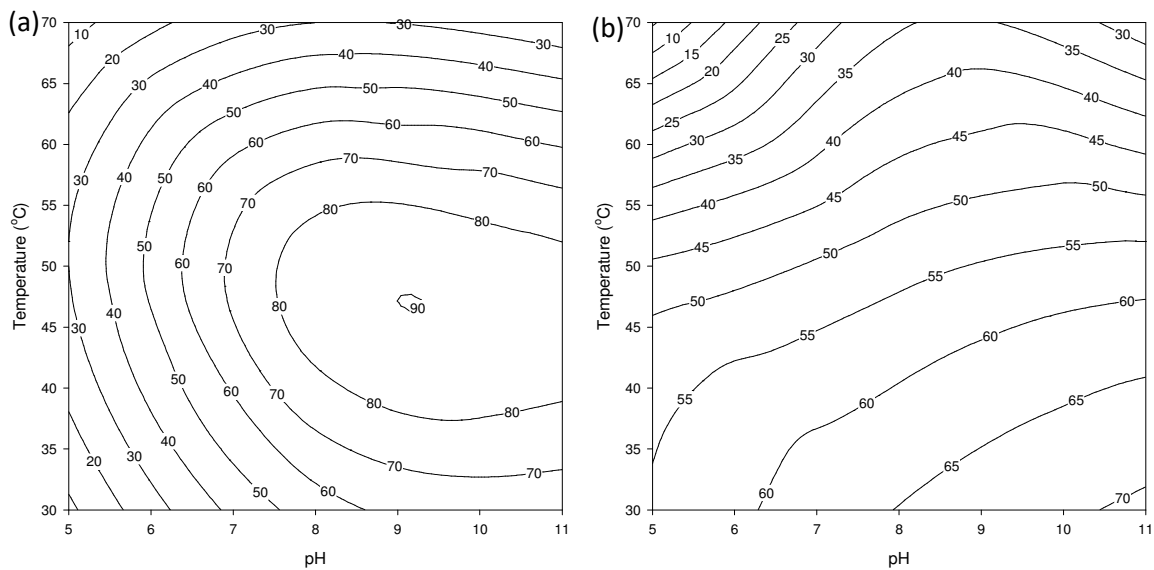
759 Fig. 5



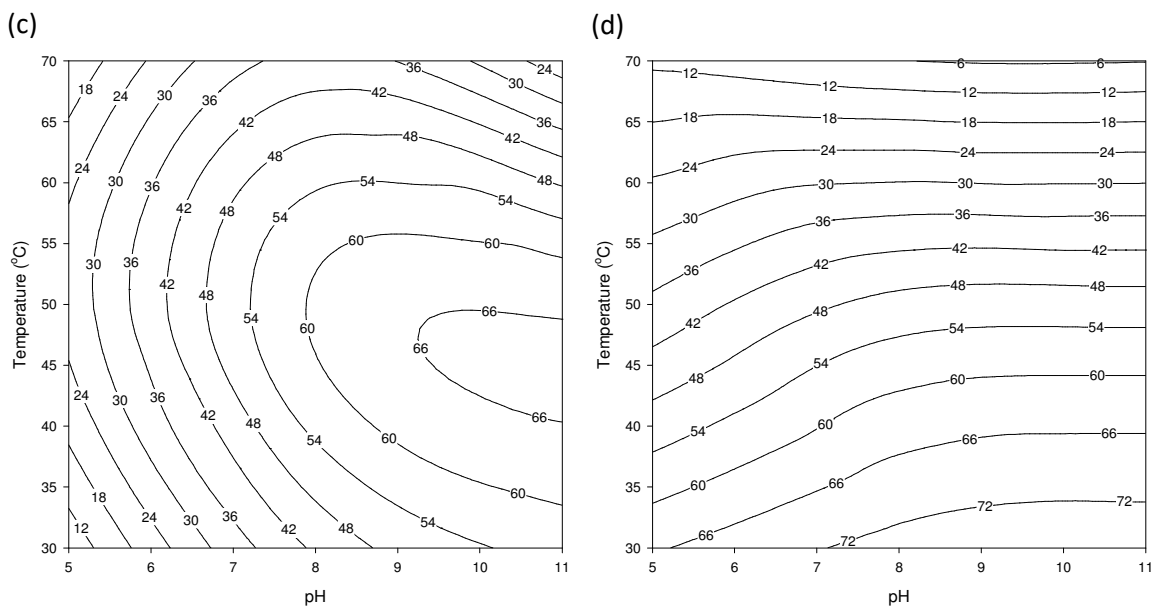
760

761

762 **Fig. 6**



763



764

765

766

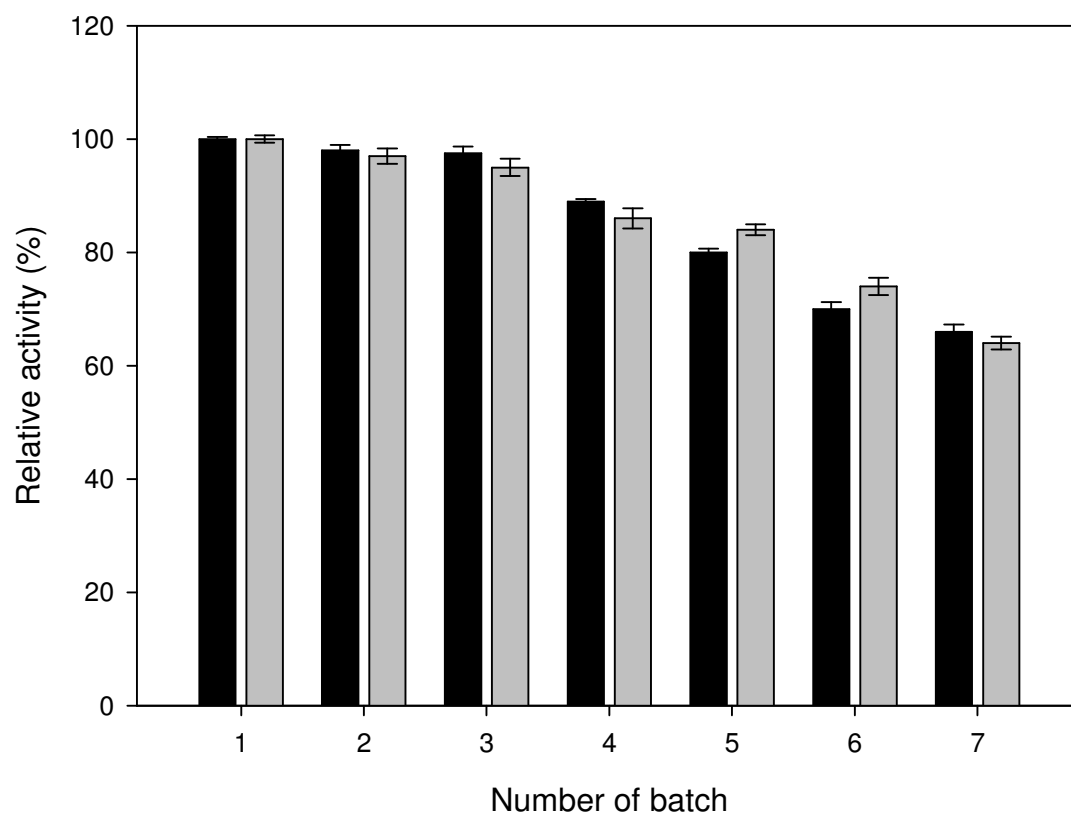
767

768

769

770

771

772 **Fig. 7**

773

774

775

776

777

778

779

780

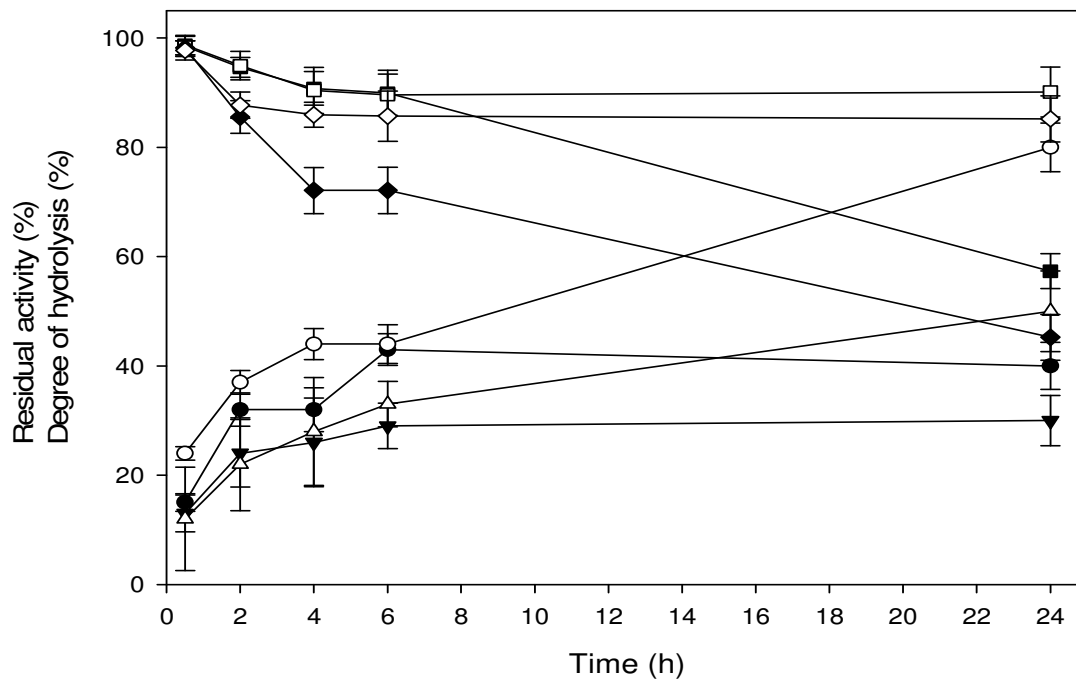
781

782

783

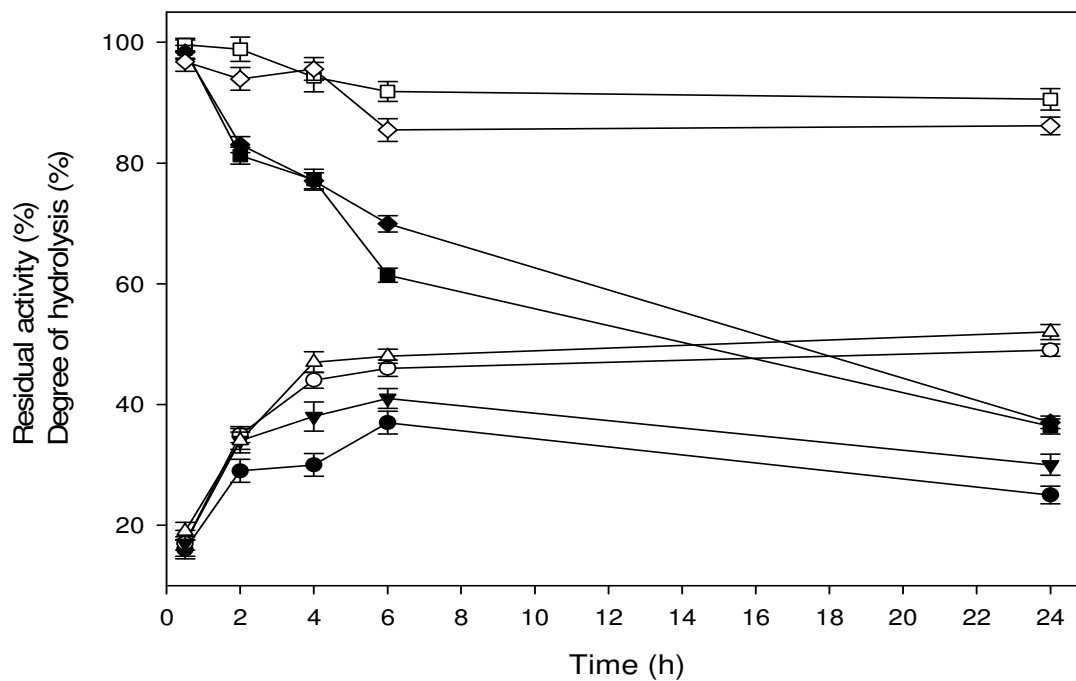
784 **Fig. 8**

(a)



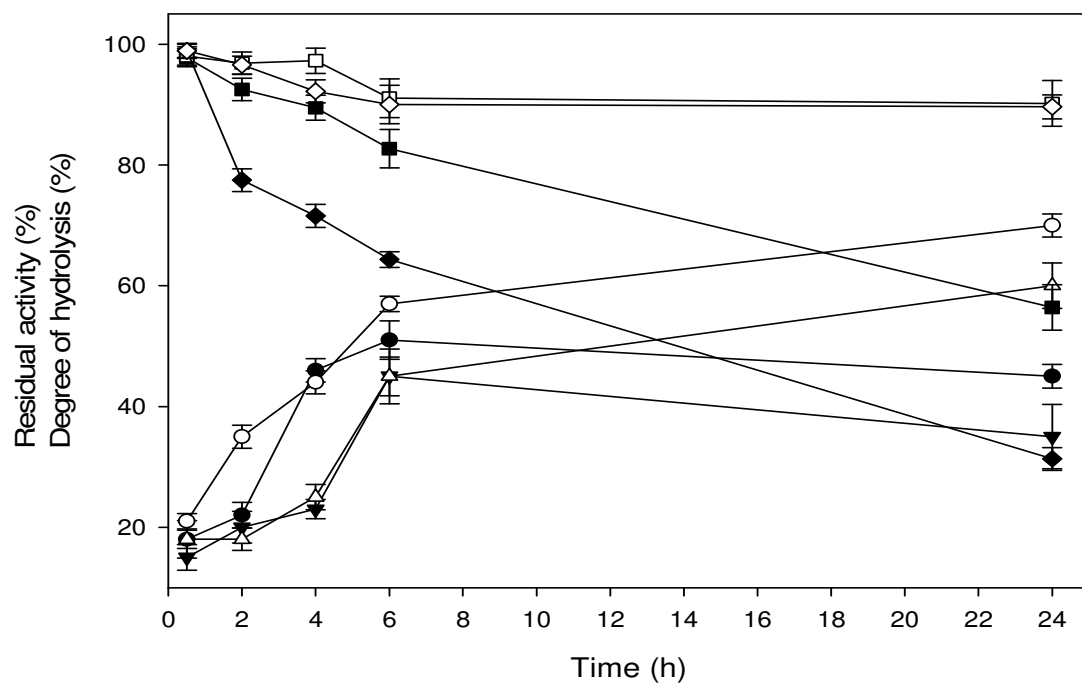
785

(b)



786

(c)



787

788

789

790

791

792

793

794

795

796

797

798

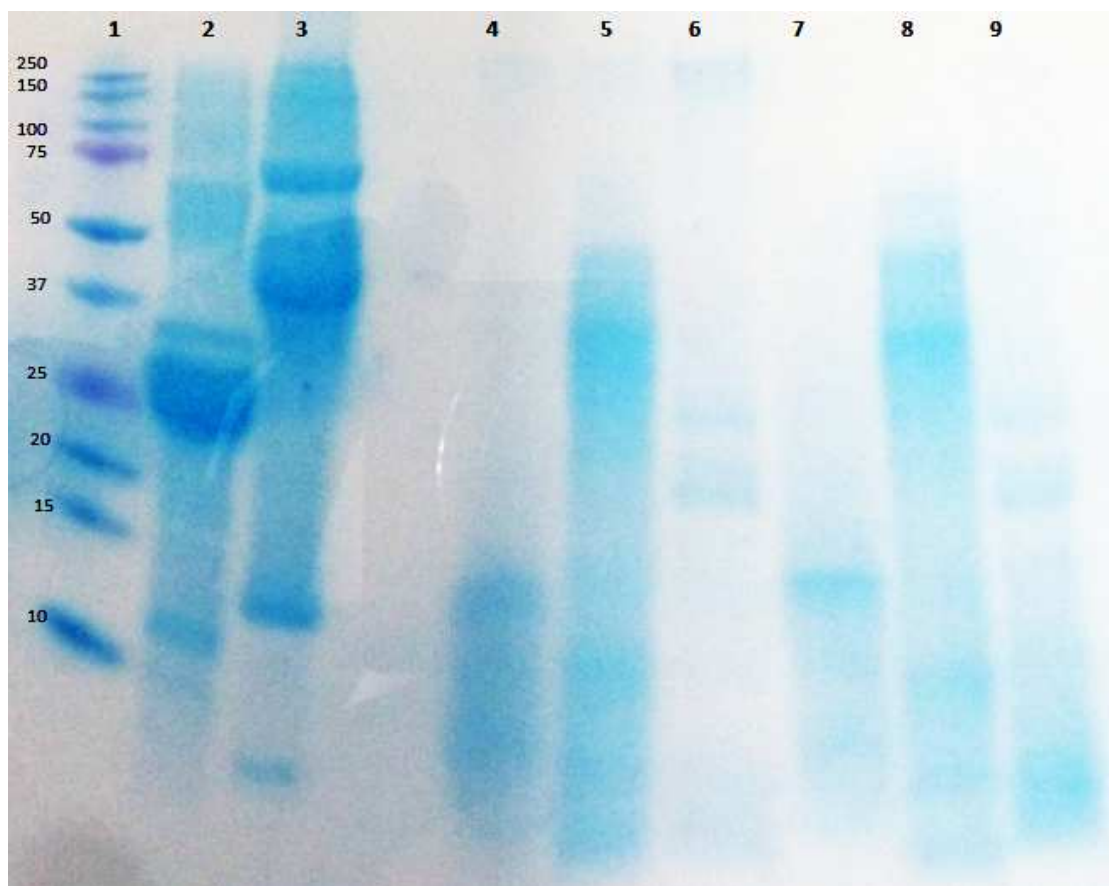
799

800

801

802 **Fig. 9**

803



804